

Response to community – Development of iron-mediated molecular chlorine chemistry in GEOS-Chem: model description, evaluation and global atmospheric implication

We are grateful for the feedback and guidance of reviewer. The comments and concerns have been addressed carefully. Exact comments from the reviewer are in black italic type. Our responses (indent and in normal font) and the corresponding edits in the manuscript (indent and in blue) are shown below.

Comments from Maarten M. J. W. van Herpen:

Chen et al. incorporate an iron-mediated molecular chlorine (Cl₂) formation mechanism into the GEOS-Chem model. They represent the dynamic solubility of iron (Fe) as a function of aerosol acidity, organic complexation, and mineralogical variability. The comparisons indicate that this newly implemented mechanism significantly improves the model's performance in simulating Cl₂ concentrations and substantially alters the global distribution of atmospheric oxidative capacity and subsequent fine particulate matter loadings. The manuscript is well-structured, the methodology is explicitly described, and the model evaluation is logically sound. The scope of this investigation is suitable for Atmospheric Chemistry and Physics. I recommend publication after the authors address the following questions.

Response in general: We thank the reviewer for the supportive and constructive suggestions.

Main comments:

1. Line 34-35: Add reference for field studies to Röckmann2024 [2].

Response 1: We have added the reference to support the statement regarding field studies in the revised manuscript, as below.

Page 1 Line 38-41 in the revised manuscript: “In particular, laboratory (Wittmer et al., 2015a; Wittmer et al., 2015b; Wittmer and Zetzsch, 2017) and field studies (Chen et al., 2024; Chen et al., 2025b; Röckmann et al., 2024) both suggest that aerosols containing soluble iron (Fe) and chloride may generate Cl₂ through Fe(III)-mediated photochemical processes, serving as a considerable additional source of Cl radicals.”

2. Line113-114: What is meant with 'fine and coarse modes'? Please specify the aerosol diameters. Was this added to the DST1 – DST4 bins described in lines 90-95, or are these separate bins?

Response 2: To represent non-dust iron (Fe), we adopted the classification scheme developed by Hamilton et al. (2019). In their framework, fine-mode Fe (encompassing Aitken and accumulation modes) is assigned the same physical properties as black carbon (BC), while coarse-mode Fe is assigned the physical properties of mineral dust. This treatment reflects that part of combustion-related Fe may be associated with fine carbonaceous particles, which are more efficiently transported and behave more similarly to BC, whereas another part may be associated with ash or mineral-like coarse residues, which are removed more rapidly and behave more similarly to dust. Following this species-mapping strategy, we divide biomass burning Fe into two

fractions in our GEOS-Chem implementation: 25% is assigned BC-like density and deposition properties, while the remaining 75% is assigned dust-like physical properties. However, unlike the modal aerosol framework used by Hamilton et al. (2019) in CESM-CAM5, GEOS-Chem generally treats aerosol species as bulk tracers (except for sea salt and dust aerosols). Therefore, the terms ‘fine’ and ‘coarse’ are used only in a broad sense to describe their assigned aerosol physical behaviors. To avoid ambiguity, we have revised the manuscript by removing the explicit diameter description and clarifying that the two fractions represent different aerosol physical properties treatments.

Page 3 Line 121-123 in the revised manuscript: “Following the methodology of Hamilton et al. (2019), Fe emissions from BB are parameterized based on a mass ratio to black carbon (Fe:BC = 0.06), with 25% and 75% of BB Fe treated with BC-like and dust-like physical properties, respectively, to approximate their different transport and removal behaviors.”

3. Line 115-116: *Anthropogenic non-BB Fe emissions are scaled to primary sulfate emissions. What is the impact of recently reduced sulfur emissions in shipping on this?*

Response 3: In our simulations, anthropogenic non-BB Fe emissions are scaled to primary sulfate emissions, which are from CEDS v2025-04 (<https://doi.org/10.5281/zenodo.15059443>). This CEDS version extends to 2023 and updates shipping fuel sulfur content by incorporating IMO sulfur-content agreements. Therefore, the effect of recent shipping sulfur reductions is implicitly reflected in the primary sulfate fields used to scale Fe emissions. We have added relevant details in the revised manuscript, as below.

Page 4 Line 124-127 in the revised manuscript: “In this study, anthropogenic non-BB Fe emissions are scaled to anthropogenic primary sulfate emissions from the Community Emissions Data System (CEDS) emission inventory which extends to 2023 and updates shipping fuel sulfur content by incorporating IMO sulfur-content agreements, assuming a fixed mass ratio of 1:30 following previous studies (Chen et al., 2024; Alexander et al., 2009).”

4. Line 126: *Can you elaborate why non-dust uses hydrophilic and hydrophobic black carbon properties, and how this is implemented. Considering the high solubility of biomass burning Fe, would that not imply at least some hydrophilic properties?*

Response 4: The properties settings for non-dust Fe follows the methodology of Hamilton et al. (2019), which assumes the properties of fine mode Fe from fires (and anthropogenic combustion) matches black carbon (BC). This assumption is reasonable since non-dust Fe is mainly associated with combustion sources and is commonly co-emitted or mixed with carbonaceous aerosols such as BC during atmospheric transport. Accordingly, we assign non-dust Fe (including soluble and insoluble Fe) the physical properties of the corresponding BC (including hydrophilic and hydrophobic BC) species in GEOS-Chem, including density and dry/wet deposition parameters. This treatment allows the simulated Fe tracers undergo more physically realistic transport and scavenging processes throughout their atmospheric residence. Regarding the high solubility of biomass burning (BB) Fe, this characteristic is represented by prescribing a relatively high soluble fraction at

emission. Specifically, we treat 20% of BB Fe as soluble Fe present at emission which is the highest among all Fe sources. The remaining 80% is emitted as insoluble which can subsequently undergo dynamic conversion to soluble Fe during transport through acidic processing and organic complexation. We have added more detailed descriptions in the revised manuscript, as below.

Page 4 Line 139-144 in the revised manuscript: “In addition, each tracer is assigned specific physical proxy properties to represent its atmospheric behaviors. Specifically, fine dust Fe follows the physical characteristics of fine-mode dust (DST1), including its prescribed density and deposition parameters. For non-dust Fe, we adopt the physical characteristics of black carbon, as these iron species are typically co-emitted and internally mixed with carbonaceous aerosols. Soluble and insoluble non-dust Fe is further mapped to hydrophilic and hydrophobic host species, respectively. This treatment ensures that the simulated Fe tracers undergo more physically reasonable atmospheric transport and scavenging processes.”

5. Line 140-145: *What are the K values used for the different dust types in the model? The authors refer to Meskhidze, who found that calcite (CaCO₃) strongly buffers deliquesced dust aerosols with a pH that remains close to 8 until the amount of acid added to the aerosol solution exceeds CaCO₃ alkalinity. The implication reported by Meskhidze is that very high intensity dust events would have very low soluble iron. It is not clear whether or how the authors have taken this into account in their model. Considering the authors only include hematite, illite and smectite in the model (Table 1), I am concerned that calcite and its effect on H⁺ is not included. That would have substantial implications for the conclusions.*

Response 5: In our implementation, the temperature-dependent rate constants $K_i(T)$ are not assigned separately to different dust types. Instead, all dust-bound Fe is treated using the slow dissolution regime, while all non-dust Fe follows the medium dissolution regime, consistent with their mineralogical stability and surface reactivity. Specifically, following Hamilton et al. (2019), the temperature-dependent rate constants are as equations R(1) and R(2):

$$K_{\text{slow}} = 1.8 \times 10^{-11} \times \exp\left(9.2 \times 10^3 \times \left(\frac{1}{298} - \frac{1}{T}\right)\right) \quad \text{R(1)}$$

$$K_{\text{medium}} = 1.3 \times 10^{-11} \times \exp\left(6.7 \times 10^3 \times \left(\frac{1}{298} - \frac{1}{T}\right)\right) \quad \text{R(2)}$$

Although Table 1 focuses on the iron-bearing minerals (hematite, illite, and smectite), the buffering effect of calcite is explicitly accounted for in our model through a mass-balance treatment of mineral-dust alkalinity. Following the methodology of Luo et al. (2008), we assume that 6% of the total mineral dust is soluble calcite. The aerosol pH is then determined by the concentration of the primary acidic species (sulfate) and the available calcite. We have added these details in the revised manuscript, as below.

Page 5 Line 167-168 in the revised manuscript: “For simplify, aerosol pH is determined by the concentration of major acidic species (sulfate) and the alkaline buffering capacity of mineral dust (calcite). Following Luo et al. (2008), we assume 6% of mineral dust is soluble calcite.”

6. Line 151: It is known from Wittmer2014 [3] that oxalate has two opposite types of impact on iron-mediated chlorine production. First, oxalate forms a stable and dominant complex with Fe(III) that diminishes the Fe(III)–Cl complexation and thus the direct activation of chloride. At the same time, the photolysis of the Fe(III)–oxalate complexes leads to a formation of H₂O₂ and this stimulates the reoxidation of Fe(II) (rate k_1 of equation 6 at line 180), accelerating the production rate of Cl₂. This creates an uncertainty for the model implementation of the IMC mechanism. The authors should discuss this in more detail, and ideally would also include a sensitivity assessment, for example through a model run that excludes ligand-mediated dissolution.

Response 6: Thanks for your insightful suggestions. We agree that the dual role of oxalate in the iron-mediated chlorine (IMC) mechanism. In the present study, however, we do not explicitly simulate the formation mechanism of oxalate. Instead, following the approach of Scanza et al. (2018) and subsequent studies (Hamilton et al., 2019), oxalate concentrations are scaled to SOA as a simplified representation. Although this treatment does not resolve the detailed formation and loss pathways of oxalate, it produces concentration levels and spatial patterns comparable to studies that using a state-of-the-art aqueous-phase chemical scheme of oxalate (Myriokefalitakis et al., 2011; Scanza et al., 2018). Within our framework, the ligand-promoted dissolution pathway represents oxalate complexing Fe(III) to prevent its precipitation, followed by the release of Fe(III) that subsequently participates in Fe–Cl complexation and IMC-driven Cl₂ formation. Under this simplified representation, oxalate acts primarily as a promoter of Fe dissolution and thus enhances Cl₂ production in this study. We acknowledge that this simplification may lead to an overestimation of the net effect of oxalate on Cl₂ formation. We have added a discussion of this uncertainty in the revised manuscript, as below.

Page 9 Line 322-324 in the revised manuscript: “Furthermore, the simplified treatment of organic ligands also introduces uncertainty which neglects the potential competitive complexation between oxalate and chloride for Fe(III). Thus, actual Cl₂ yield may be overestimated under certain environmental conditions.”

7. Line 182-183: The rate k_1 of equation 6 is based on VanHerpen2023, who based this rate on a typical aerosol H₂O₂ concentration of 50 μM. A suggestion for an improvement to the mechanism is to make k_1 dependent on modelled H₂O₂ concentrations in GEOS-Chem. I understand that this suggestion might be beyond the scope of the current work, but if the authors would consider this improvement, it would add important additional value to the manuscript.

Response 7: We completely agree with your suggestion that making k_1 (the reoxidation rate of Fe(II)) dependent on modelled H₂O₂ concentrations would significantly enhance the representation of the IMC mechanism. However, as discussed in Response 6, since the current study does not explicitly simulate the dynamic photochemical cycle of oxalate, we have maintained the k_1 parameterization based on the constrained values from van Herpen et al. (2023) to ensure internal consistency within the current model framework. We recognize this as a high-priority direction for future model development. Incorporating the coupling between k_1 and H₂O₂, especially alongside an explicit oxalate module, would provide a more comprehensive evaluation of the dual role of organic ligands in chlorine activation. We have added a new section, “Text S2 Other potential

uncertainty analysis.”, to the revised supplementary materials to highlight this potential improvement, and the corresponding statement has also been included in the revised manuscript, as below.

Page 9 Line 324 in the revised manuscript: “Other potential uncertainties are discussed in Text S2 in the supplementary materials.”

Page 11 in the revised supplementary materials: “The treatment of the Fe(II) reoxidation rate constant k_1 also introduces uncertainty into the current IMC parameterization. In this study, k_1 is prescribed following Van Herpen et al. (2023), where the value is constrained using a typical aerosol H_2O_2 concentration of $50 \mu\text{mol L}^{-1}$. This simplified treatment does not explicitly account for the spatial and temporal variability of H_2O_2 simulated in GEOS-Chem, which may influence the Fe(II)/Fe(III) cycling rate and thus the efficiency of IMC-driven Cl_2 production. In addition, since the present model does not explicitly resolve the dynamic photochemical cycling of oxalate, the coupled effects of H_2O_2 , organic ligands, and Fe redox cycling remain simplified. Future development could improve this mechanism by making k_1 dependent on modelled H_2O_2 concentrations and by coupling it with an explicit oxalate module to better represent the chemical controls on iron-mediated chlorine activation.”

8. Line 225 (results section): Can the authors provide total Cl_2 production values for the different Fe sources? In other words, what Fe source from Table 1 is the main contributor to Cl_2 production?

Response 8: Thanks for this comment. Following Table 1 in the manuscript, we classified Fe into three source categories including dust Fe, biomass-burning Fe, and other anthropogenic Fe, and quantified their respective contributions. The global annual Cl_2 production attributable to each Fe source is shown in Fig. R1. As illustrated in Fig. R1, dust Fe overwhelmingly dominates global Cl_2 production, consistent with its large mass contribution and widespread spatial coverage. Biomass-burning Fe provides a secondary but regionally significant contribution, particularly over boreal fire regions, the Amazon, central Africa, and Southeast Asia. Anthropogenic Fe contributes the least, with noticeable impacts only in densely populated industrial regions.

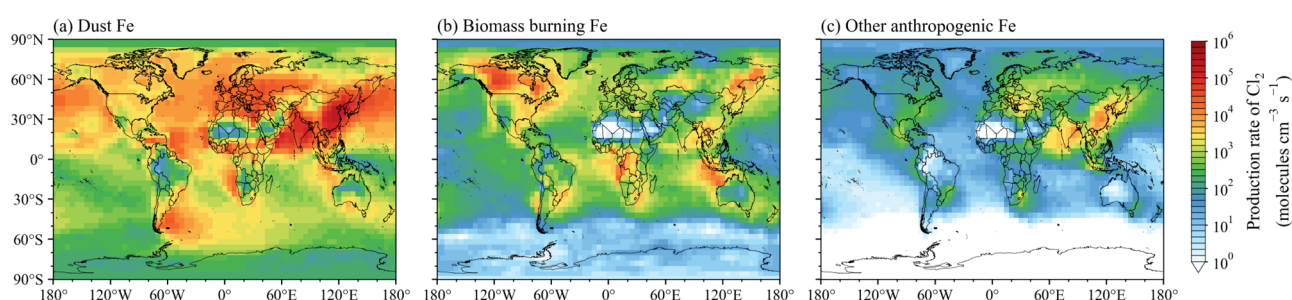


Figure R1. Source-specific spatial distributions of annual mean Cl_2 production rate attributable to (a) dust Fe, (b) biomass-burning Fe, and (c) other anthropogenic Fe.

A new figure showing the Cl_2 production rate attributable to Fe from different sources has been added to the revised supplementary materials (as Fig. S7), and the corresponding discussion has been incorporated into the revised manuscript, as below.

Page 10 Line 341-342 in the revised manuscript: “Consistently, the source-specific attribution analysis indicates that biomass-burning Fe provides a regionally important contribution to Cl₂ production over WC (Fig. S7).”

Page 10 Line 350-351 in the revised manuscript: “In contrast to these regions, Cl₂ maxima over the TA are governed by the long-term background input of natural mineral dust Fe (Fig. S7).”

9. Line 266: *I don't agree with the authors that the ~30% magnitude of Cl₂ concentrations reflects the inability for the FixFeS scenario to represent realistic photoactive Fe abundances in certain regions, because an increase in the reaction rates of equation 6 would increase it in line with the observations. Thus, the lower Cl₂ concentrations are more likely indicating an underestimation of the rates in equation 6. Instead, I would agree if the authors would use the correlation coefficient to argue for better performance by the VarFeS scenario.*

Response 9: Thanks for your critical comment. We agree that the Cl₂ concentrations underestimation for the ‘FixFeS’ scenario could potentially be mitigated by scaling the reaction rates of Equation 6. In addition to the simulated magnitude, we used the correlation coefficient to evaluate the spatial and temporal consistency between the model and observations. The higher correlation in ‘VarFeS’ scenario (r=0.88) compared to ‘FixFeS’ scenario (r=0.74) indicates that incorporating process-based, variable iron solubility better captures the observed variability in Cl₂. We have adjusted our description in the revised manuscript, as below.

Page 8 Line 301-303 in the revised manuscript: “In the “FixFeS” scenario, a fixed 1.8 % fraction of photoactive Fe also results in a lower correlation with observations (r = 0.74) compared with “VarFeS” scenario. This discrepancy reflects the inability of a constant fraction to represent the realistic spatial variability of soluble Fe abundances.”

10. Line 265: *The fixed 1.8% fraction is based on the assumption that the photoactive fraction is not the same as soluble fraction, but it is the fraction of soluble iron that can be oxidized and reduced repeatedly (VanHerpen2023). This is represented by the FixFeS scenario in the manuscript. The VarFeS scenario assumes that photoactive fraction is equal to the soluble fraction. However, the sentence at line 265 that refers to “photoactive Fe reaches 32%” should be rephrased to “soluble Fe reaches 32%”, because the number reported in the reference is the total soluble iron fraction.*

Response 10: Thank you for this comment. We have revised “photoactive Fe reaches 32%” to “soluble Fe reaches 32%” in the revised manuscript to avoid ambiguity. We also would like to clarify that, in the “FixFes” and “VarFeS” simulation, dissolved Fe is used as a proxy for the Fe pool available for IMC-driven Cl₂ production. The potential overestimation associated with this assumption has been further discussed in the uncertainty section. We have modified our phrasing to avoid misunderstanding in the revised manuscript, as below.

Page 6 Line 214-218 in the revised manuscript: “The “FixFeS” simulation includes the IMC mechanism with a uniform fraction of 1.8 % for photoactive soluble iron, following the ratio treatment of photoactive Fe in

Van Herpen et al. (2023). The “VarFeS” simulation incorporates both the IMC mechanism and a dynamic representation of iron solubility modulated by proton processing, organic complexation, and mineralogical variability. Since the fraction of dissolved Fe that is photochemically active is not well constrained, we use dissolved Fe as a proxy for the Fe pool available for IMC-driven Cl₂ production.”

Page 8 Line 303-305 in the revised manuscript: “This is supported by the fact that Fe solubility itself exhibits significant regional heterogeneity. For instance, observed soluble Fe fractions can reach as high as 32% in the North Atlantic due to anthropogenic pollutants from North America and Europe (Chen and Siefert, 2004).”

Page 9 Line 316-318 in the revised manuscript: “The use of soluble Fe as a surrogate for photoactive Fe may also contribute to this positive bias, as only a fraction of dissolved Fe may effectively participate in photochemical Fe cycling.”

11. Line 283: change “global mean Cl₂ concentrations” into “global mean surface Cl₂ concentrations”.

Response 11: We have revised the manuscript, as below.

Page 9 Line 329-331 in the revised manuscript: “As illustrated in Fig. 3, the inclusion of the IMC mechanism induces a profound shift in global mean surface Cl₂ concentrations, which increases from 0.4 (with a range of 0-11) pptv in the “Base” scenario to 2.2 (with a range of 0.01-57) pptv in the “VarFeS” scenario.”

12. Line 299: Can the authors elaborate on this, because both the production (eq6) and the loss (photolysis) are depending on solar radiation. Weakened solar radiation would therefore reduce both Cl₂ production and Cl₂ photolysis at the same time, so why would this explain accumulation of Cl₂ at the surface?

Response 12: Thank you for this insightful comment. We agree that solar radiation is important for both Cl₂ production and loss and we cannot isolate this influence in our current model configuration. During wintertime, anthropogenic iron and chlorine emissions are considerably higher due to increased coal combustion and biomass burning for residential heating and industrial activities. Substantial emissions of HCl, particulate Cl⁻, and chlorine-containing organics provide a more abundant chlorine reservoir for IMC chemistry. As a result, the potential for Cl₂ formation remains elevated even when solar radiation is weak, consistent with the higher wintertime Cl₂ levels simulated over the NCP and northern India where anthropogenic chlorine emissions are particularly pronounced. Furthermore, winter meteorological conditions amplify this accumulation. Shallow boundary layers, stagnant conditions, and weak vertical mixing significantly limit the dispersion of Cl₂ and its precursors, allowing it to remain trapped near the surface. We have modified our discussion in the revised manuscript, as below.

Page 10 Line 345-347 in the revised manuscript: “Combined with wintertime meteorological synergies, such as shallow planetary boundary layer heights and frequent stagnant conditions that suppress vertical dispersion, these factors collectively lead to the persistent accumulation of Cl₂ in the surface layer.”

13. Line 305: Could the authors include in the supplemental information a figure that shows Cl₂ production rate (molec/cm³/s). This helps the reader distinguish between production effects and loss effects for Cl₂.

Response 13: We have added a figure to display the Cl₂ production rate in the revised supplementary materials (as Fig. S8), as below.

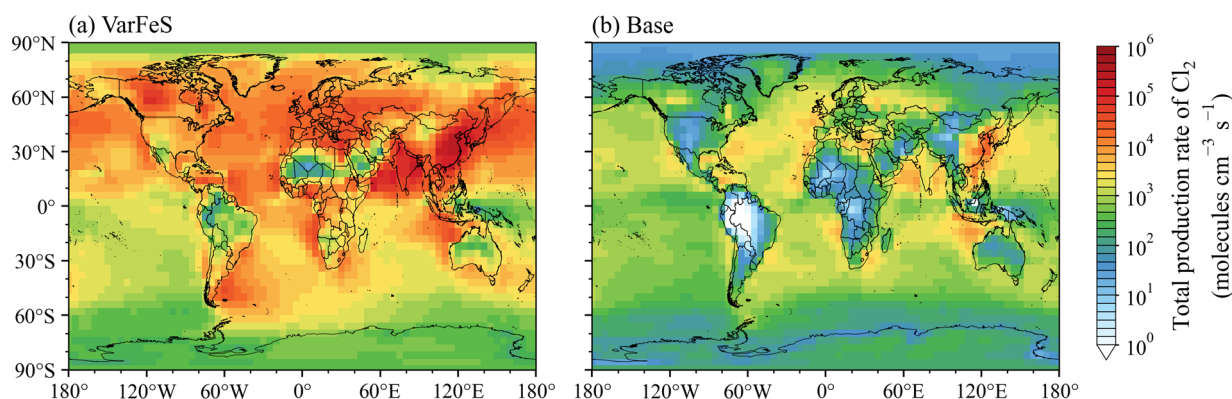


Figure R2. Spatial distributions of annual mean total Cl₂ production rate under different simulation scenarios (a, b)

Related statement has also been added in the revised manuscript, as below.

Page 12 Line 419-422 in the revised manuscript: “Furthermore, as noted by Pennacchio et al. (2025), the impact of Cl₂ is non-linearly dependent on its production intensity as well. In the NCP, which represents the highest Cl₂ production rate hotspot in our study (as shown in Fig. S8), chlorine-mediated radical chemistry may provide additional pathways (e.g., through the Cl + CH₃OOH reaction) for OH formation beyond the conventional NO-driven HO₂-to-OH conversion.”

14. Line 332: *The authors should refer to Pennacchio2025 [4] in this section, where the effects of Cl₂ emission on atmospheric oxidation capacity have been investigated, including the role of NO_x and ozone. Pennacchio2025 reported that ClONO₂ hydrolysis is an important reaction that influences AOC. Do the authors see the same in the GEOS-Chem model output?*

Response 14: Thanks for your helpful suggestions. We have now incorporated this reference and expanded our discussion on the effects of the IMC mechanism on atmospheric oxidative capacity (AOC). Specifically, we added discussion on the NO_x- and O₃-dependent response of Cl₂-driven oxidation chemistry. Pennacchio et al. (2025) demonstrated that ClO_x chemistry can suppress OH production by depleting O₃ and NO₂ under low-to-moderate NO_x conditions, whereas sufficiently high Cl₂ production can introduce additional OH sources and enhance radical recycling through chlorine-mediated reactions. This provides useful mechanistic support for our simulated regionally differentiated AOC responses, including the global decrease in OH and O₃ over low-NO_x remote regions and the localized enhancement of OH and O₃ over the North China Plain. Related discussions have been supplemented to the revised manuscript, as below.

Page 11 Line 394-396 in the revised manuscript: “It should be noted that the simulated RO₂ enhancement does not necessarily imply a uniform enhancement of AOC, as the subsequent oxidant response is strongly dependent on local NO_x and O₃ conditions (Pennacchio et al., 2025).”

Page 11 Line 405-407 in the revised manuscript: “A similar mechanism was highlighted by Pennacchio et al. (2025), who demonstrated that Cl₂-driven chemistry can suppress OH production by reducing O₃ and NO₂ under low-to-moderate NO_x conditions, despite enhanced chlorine radical production.”

Page 12 Line 419-423 in the revised manuscript: “Furthermore, as noted by Pennacchio et al. (2025), the impact of Cl₂ is non-linearly dependent on its production intensity as well. In the NCP, which represents the highest Cl₂ production rate hotspot in our study (as shown in Fig. S8), chlorine-mediated radical chemistry may provide additional pathways (e.g., through the Cl + CH₃OOH reaction) for OH formation beyond the conventional NO-driven HO₂-to-OH conversion. This intensity-dependent response further helps explain the sharp contrast in OH variations between the NCP and other regions.”

Regarding the influence of ClONO₂ hydrolysis to AOC, our GEOS-Chem simulations indeed show an enhancement in ClONO₂ concentrations following the inclusion of the IMC mechanism (as shown in Fig. R3). This enhancement spatially correlates with the regions where significant declines in O₃ are predicted. This consistency supports the mechanism proposed by Pennacchio et al. (2025), suggesting that ClONO₂ formation and its subsequent heterogeneous loss act as a critical sink for both NO_x and O₃, thereby suppressing the overall atmospheric oxidative capacity in these environments. While our current model output aligns with the qualitative findings of Pennacchio et al. (2025), a precise quantitative attribution of the AOC change to the ClONO₂ hydrolysis pathway specifically would require additional targeted sensitivity simulations and diagnostic budget analyses. In the present work, we have prioritized assessing the overall impact of Fe(III)-mediated Cl₂ formation as a newly integrated process in GEOS-Chem, thus a more detailed pathway-specific budget analysis will be a key focus of our future research. We have added a discussion in the revised manuscript noting the ClONO₂ enhancement and its potential role in O₃ decline, as below:

Page 12 Line 429-431 in the revised manuscript: “This decline is further exacerbated by the formation of ClONO₂ (as shown in Fig. S9) via the reaction of ClO with NO₂ and its subsequent hydrolysis which acts as an efficient sink of NO_x thereby substantially suppresses O₃ photochemical production (Pennacchio et al., 2025).”

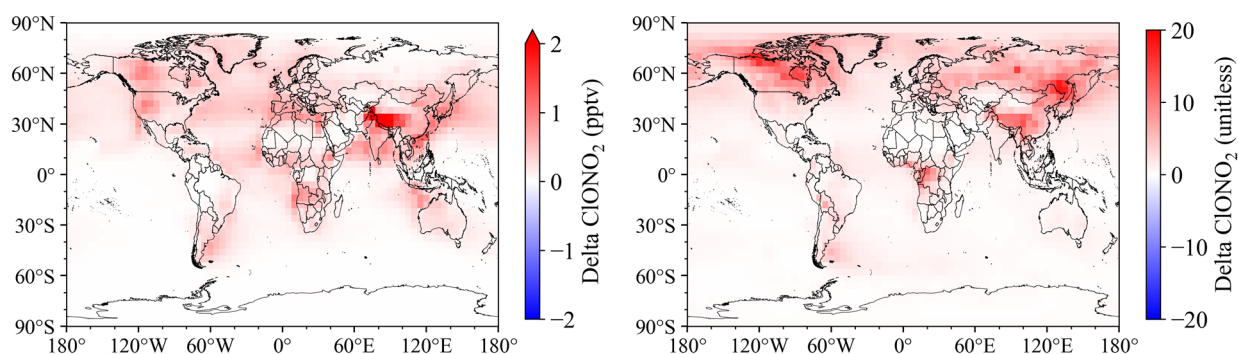


Figure R3. Comparison of absolute changes (left: VarFeS-Base) and relative changes (right: (VarFeS-Base)/Base) in annual mean surface concentration of ClONO₂.

15. Line 365: *Following Pennacchio2025, the impacts of Cl₂ emission are strongly depending on the local intensity of Cl₂ emissions. This can explain part of the difference between the NCP region and other regions, because the NCP region has the highest intensity of Cl₂ emissions.*

Response 15: Thanks for this insightful comment. We now explicitly state that the exceptional O₃ enhancement in the NCP is not only due to high NO_x levels but also driven by its massive Cl₂ production intensity. According to the “high-chlorine regime” proposed by Pennacchio et al. (2025), higher Cl₂ production may provide additional pathways (e.g., through the Cl + CH₃OOH reaction) for OH formation. This further clarifies why the NCP stands out as a unique region for radical enhancement compared to other global areas. We have added some discussions in the revised manuscript, as below.

Page 12 Line 419-423 in the revised manuscript: “Furthermore, as noted by Pennacchio et al. (2025), the impact of Cl₂ is non-linearly dependent on its production intensity as well. In the NCP, which represents the highest Cl₂ production rate hotspot in our study (as shown in Fig. S8), chlorine-mediated radical chemistry may provide additional pathways (e.g., through the Cl + CH₃OOH reaction) for OH formation beyond the conventional NO-driven HO₂-to-OH conversion. This intensity-dependent response further helps explain the sharp contrast in OH variations between the NCP and other regions.”

Page 12 Line 435-443 in the revised manuscript: “Under NO_x-excess conditions, the particularly high local Cl₂ production rate over the NCP likely further amplifies this positive O₃ response (Fig. S8). Acceleration of VOCs oxidation by Cl radicals substantially increases RO₂ concentrations and thereby promotes photochemical O₃ production, overcompensating for any NO_x loss via ClONO₂ pathways. By contrast, although India experiences comparable NO_x levels and elevated Cl₂ concentrations to those in NCP, a slight decrease in O₃ concentration is observed due to its distinct O₃ photochemical regime. Recent satellite evidence confirms that the majority of India predominantly resides within a “NO_x limited regime” with respect to ozone formation (Pakkattil and Ghude, 2025; Rawat and Naja, 2022). Consequently, the combination of chlorine-driven NO_x depletion together with the direct consumption of O₃ by Cl leads to decreased O₃ levels over India.”

16. Line 385: *While the authors are discussing increased PM_{2.5} in certain regions, they fail to point out that in other regions the PM_{2.5} decreases. The authors note that the reason for the PM_{2.5} increase in the NCP region is the accelerated conversion of nitrogen oxides into nitrate (line 393). What the authors should include in this discussion is that this also implies that PM_{2.5} is reduced in other locations. This is visible in Figure 6, which shows reduced PM_{2.5} downstream of the NCP region. This is an important finding, because it means that the location of chlorine enhancement will determine whether air quality improves or declines in certain population zones. Or in other words, it appears PM_{2.5} is not increased globally, but instead it is displaced geographically.*

Response 16: Thanks for this critical comment. We have expanded our discussions about the decreasing tendency of PM_{2.5}, as below.

Page 13 Line 470-484 in the revised manuscript: “In contrast, regions located downwind of the enhanced Cl₂ production zones, as well as adjacent marine areas, exhibit a general decrease in PM_{2.5} concentrations. This

reduction is likely attributable to the accelerated oxidation of NO_x and other precursors near the source regions under strengthened AOC. As NO_x is more rapidly converted to HNO₃ and subsequently to particulate nitrate, these species undergo earlier deposition and removal, thereby diminishing the reservoir of precursors available for long-range transport and secondary aerosol formation. Consequently, the downwind regions experience lower PM_{2.5} levels. In addition, this decreasing pattern is also consistent with the spatial distribution of sulfate reductions (Fig. S10). Under conditions of enhanced HO_x cycling, nitrate and sulfate do not respond uniformly to the IMC mechanism. While nitrate formation is strongly driven by increased OH oxidation (Liu et al., 2020; Wang et al., 2026), sulfate production is governed not only by gas-phase OH oxidation of SO₂ but also by aqueous, heterogeneous, and transition-metal-catalyzed oxidation pathways (Guo et al., 2024; Gao et al., 2024; He et al., 2025). Besides, hydroxymethanesulfonate (HMS) formed through the reaction between dissolved SO₂ and HCHO can subsequently be oxidized by aqueous OH radicals to sulfate (Song et al., 2019, Ma et al., 2020, Dovrou et al., 2022). Though elevated regional OH levels promote HCHO production which further increases the concentration of HMS (Fig.S12), HMS formation may temporarily sequester precursor SO₂, and its subsequent oxidation is likely insufficient to offset the suppression of sulfate formation via direct SO₂ oxidation. Therefore, sulfate concentrations slightly decrease over the NCP despite the enhanced OH levels.”

17. Line 385: *The model uses only a short spin-up period of 6 months. For the conversion of nitrogen oxides into nitrate this is sufficient spin-up time. However, is it sufficient to create a stable state for other important mechanisms that produce fine particle matters?*

Response 17: Thanks for your insightful comment. To address this concern, we conducted an additional sensitivity simulation with a 1-year spin-up period and compared the PM_{2.5} responses induced by the Fe(III)-mediated Cl₂ formation mechanism under the two spin-up settings. As shown in Fig. R4, the absolute PM_{2.5} changes between ‘VarFeS’ and ‘Base’ scenarios are highly consistent between the 6-month and 1-year spin-up simulations, with the vast majority of regions showing negligible deviations, indicating that the mechanism-induced PM_{2.5} perturbation is not sensitive to extending the spin-up period from 6 months to 1 year. Therefore, we believe the 6-month spin-up duration is acceptable for this study.

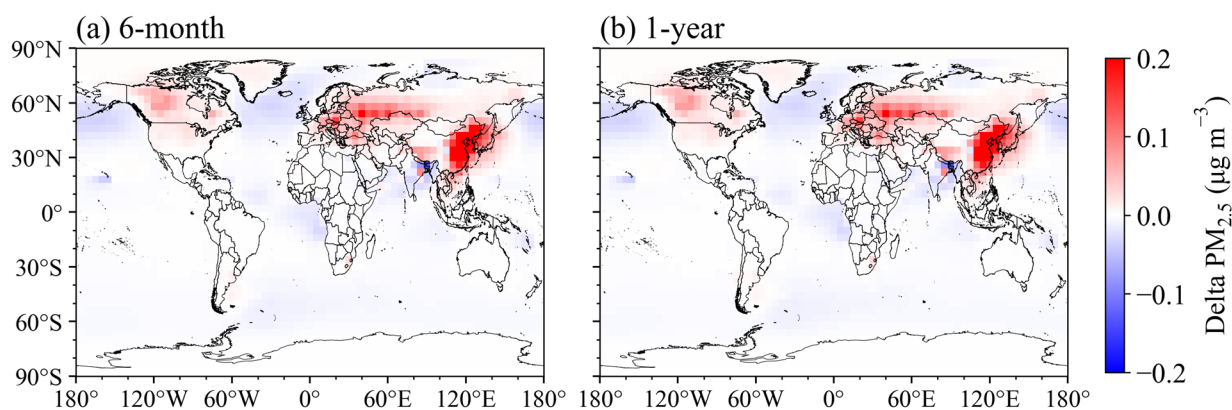


Figure R4. Comparison of absolute changes (VarFeS-Base) of PM_{2.5} for (a) 6-month and (b) 1-year spin-up simulations.

18. Line 417: *The conclusions should note that $PM_{2.5}$ is also reduced elsewhere. E.g. the conclusion could be rephrased to say “with localized $PM_{2.5}$ surges reaching 6%, while $PM_{2.5}$ is reduced downstream.”*

Response 18: Thanks for this comment. We have rephrased our statement in the conclusion section, as below.

Page 14 Line 507-508 in the revised manuscript: “This effect is further intensified during stagnant winter episodes, with localized $PM_{2.5}$ surges reaching 6 %, while $PM_{2.5}$ is reduced downstream.”

19. Line 20 (abstract): *Similar to my comments on $PM_{2.5}$ above, the authors should also rephrase line 20 in the abstract to include that $PM_{2.5}$ is reduced downstream of the region with enhanced AOC.*

Response 19: Thanks for this comment. We have rephrased our statement in the abstract section, as below.

Page 1 Line 21-22 in the revised manuscript: “Conversely, a discernible decline in $PM_{2.5}$ occurs in the downwind regions with enhanced AOC and also remote marine regions.”

20. Line 403: *There are two relevant studies that implemented an iron-mediated chlorine production mechanism in a global model, to which the authors should compare their result. The first one is Chen2024 [5] from the same group as the current manuscript, but uses a very different mechanism. The second study is Meidan2024 [6], who also implemented an IMC mechanism combined with iron dissolution.*

Response 20: Thanks for pointing out these two relevant studies. Chen et al. (2024) implemented an Fe(III)-mediated Cl_2 formation mechanism in GEOS-Chem and evaluated the model performance against Cl_2 observations at the Wangdu site in North China. Overall, the conclusions of the two studies are consistent: gas-phase and heterogeneous Cl_2 formation mechanisms substantially underestimate observed Cl_2 concentrations, whereas the inclusion of Fe(III)-mediated Cl_2 production markedly improves the model representation of Cl_2 and further affects regional reactive chlorine cycling and atmospheric oxidative capacity.

Specifically, at the Wangdu site, Chen et al. (2024) reported observed mean Cl_2 mixing ratios of 48 ± 51 pptv during the daytime and 28 ± 35 pptv at night. In their “RUNFe” simulation, the modeled Cl_2 was approximately one-third of the observed daytime mean and one-half of the observed nighttime mean, indicating that their Fe(III)-mediated mechanism substantially improved the Cl_2 simulation but still did not fully capture the daytime high values. This remaining underestimation may be related to the empirical nature of their parameterization, which explicitly depends on jNO_2 , Fe(III), aerosol chloride, and aerosol surface area. As noted by Chen et al. (2024), Fe(III), aerosol chloride, and aerosol surface area are still subject to observational constraints and model uncertainties. In addition, aerosol pH was not explicitly included in their parameterization, although pH can regulate Fe speciation and the partitioning between Fe(III)-Cl and Fe(III)-hydroxy complexes, thereby affecting the efficiency of Fe(III)-mediated Cl_2 production. These factors may partly contribute to the remaining low bias in Chen et al. (2024). In our study, the corresponding monthly mean Cl_2 mixing ratio at Wangdu site is 58.5 pptv, which is broadly consistent with the observed daytime mean but higher than the observed nighttime mean. Since our simulation was conducted at a global resolution to examine the large-scale

impacts of Fe-mediated Cl₂ production on reactive chlorine chemistry, atmospheric oxidative capacity, and air quality, the grid-cell-mean aerosol composition, aerosol surface area, soluble Fe concentration, and aerosol chloride concentration in our simulation are not directly comparable to those in the high-resolution nested simulation of Chen et al. (2024). In addition, as discussed in Section 3.1.2, the relatively high Cl₂ level in our simulation may also be associated with uncertainties in the current Fe(III)-mediated Cl₂ formation parameterization, including the use of regionally constrained empirical rate constants, the idealized treatment of Cl₂ production efficiency, and the simplified representation of competitive radical quenching and Fe-organic ligand complexation. We have added a discussion for this discussion in the revised manuscript, as below.

Page 9 Line 307-324 in the revised manuscript: “In comparison with the previous nested GEOS-Chem study over North China by Chen et al. (2024), both studies consistently show that traditional gas-phase and heterogeneous Cl₂ formation mechanisms substantially underestimate observed Cl₂, while IMC mechanism markedly improves model performance. At the Wangdu site, Chen et al. (2024) reported observed mean Cl₂ mixing ratios of 48 ± 51 pptv during the daytime and 28 ± 35 pptv at night, while their ‘RUNFe’ simulation reproduced approximately one-third of the observed daytime mean and one-half of the nighttime mean. In this study, the monthly mean Cl₂ mixing ratio at the Wangdu site is 58.5 pptv, broadly consistent with the observed daytime magnitude but higher than the nighttime mean. This overestimation may result from the inherent limitations of the IMC parameterization. Since the rate constants k_1 and k_2 adopted in this study are derived from field measurements conducted in the North Atlantic (Van Herpen et al., 2023), so extending these regional constrained empirical parameters to a global scale may introduce inherent uncertainties, as the chemical composition and aging of aerosols vary geographically. The use of soluble Fe as a surrogate for photoactive Fe may also contribute to this positive bias, as only a fraction of dissolved Fe may effectively participate in photochemical Fe cycling. In addition, the current IMC parameterization also implicitly assumes a 100% conversion efficiency, where every two Fe(III)/Fe(II) photoactivate cycle yield one Cl₂ molecule production (as reflected in the stoichiometric factor). However, photo-induced electrons or intermediate species (e.g., Cl radicals) may undergo competitive quenching or side reactions with other reducing constituents such as organic matter or reduced sulfur species. Furthermore, the simplified treatment of organic ligands also introduces uncertainty which neglects the potential competitive complexation between oxalate and chloride for Fe(III). Thus, actual Cl₂ yield may be overestimated under certain environmental conditions.”

For Meidan et al. (2024), the treatment of Fe in their study is conceptually consistent with ours, as both studies identify soluble Fe as a key controlling factor for Fe(III)-mediated Cl₂ production and adopt a framework that accounts for the dynamic evolution of Fe solubility. Meidan et al. (2024) used the MIMI iron module in CESM2 to simulate the emissions, transport, deposition, acid processing, and organic processing of dust and combustion Fe, thereby deriving the time-varying distribution of soluble Fe. Similarly, the present study introduces a source-dependent and dynamically evolving Fe solubility scheme that considers the effects of mineralogy, acid processing, and organic complexation on soluble Fe. Therefore, both studies highlight the importance of process-based Fe solubility representations, rather than fixed Fe solubility assumptions, for

evaluating Fe-mediated chlorine activation.

However, Meidan et al. (2024) mainly focused on the potential effects of idealized Fe addition scenarios on Cl_2 production, CH_4 removal, and climate forcing. Their approach used an asynchronous modeling framework, in which soluble Fe was first simulated by CESM2-MIMI, Fe(III)-derived Cl_2 production was then diagnosed offline based on soluble Fe concentrations and photochemical assumption, and the resulting Cl_2 source was finally introduced into CESM1-CAM4 as a diurnally varying surface emission to evaluate CH_4 and radiative forcing responses. In contrast, the present study implements Fe(III)-mediated Cl_2 production within GEOS-Chem and focuses on the effects of this mechanism on Cl_2 concentrations, reactive chlorine cycling, atmospheric oxidative capacity, O_3 , and $\text{PM}_{2.5}$. Therefore, a direct quantitative comparison with Meidan et al. (2024) is not feasible based on their published diagnostics. We have added the findings of Meidan et al. (2024) to the ‘Introduction’ section to acknowledge this important previous global modelling study of Fe(III)-mediated chlorine activation, as below.

Page 2 Line 58-61 in the revised manuscript: “Recently, Meidan et al. (2024) has conducted the first global-scale attempt to link iron and Cl_2 production using an asynchronous modelling framework with a more physically based treatment of iron dissolution. However, in their configuration, the online feedbacks between iron dissolution, chlorine activation, atmospheric oxidants, and secondary aerosol formation remain incompletely represented.”

21. *Supplemental information: Figure S5: Adjusting the color scale of the top of the figure will improve visibility. Also, can the authors also include a list of Cl_2 observations in the supplemental info?*

Response 21: Following this comment, we have optimized the color scale and layout of Fig. S5 (as shown in below, now Fig. S10 in revised supplemental materials) and other figures to enhance clarity and visibility, including adjusting the color limits and increasing the font sizes for better readability. Additionally, a detailed list of Cl_2 observations has already provided in Table S2 in the supplemental material.

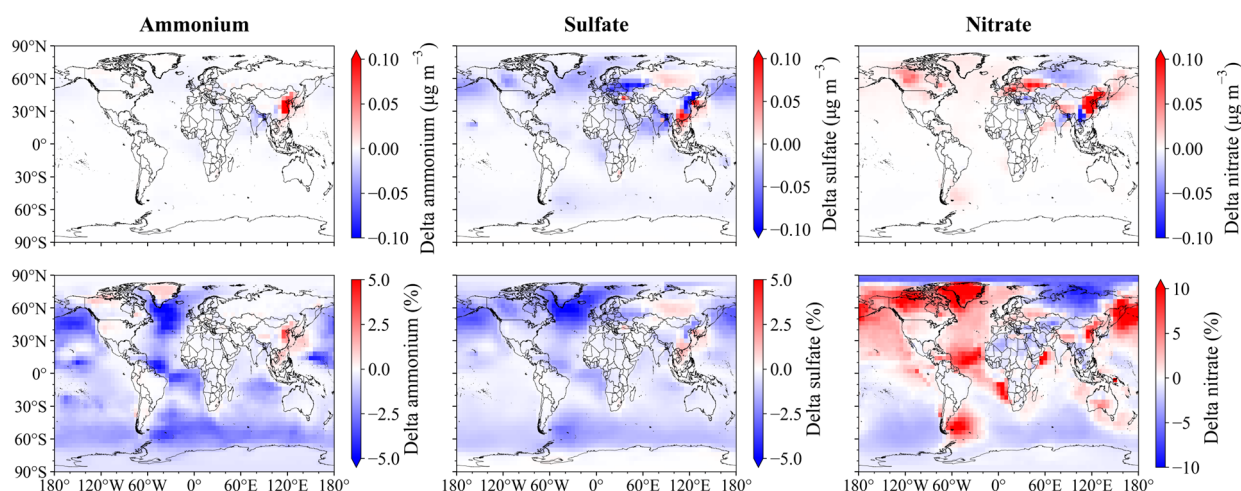


Figure R5. Differences in surface annual mean concentrations of ammonium, sulfate, and nitrate between the “VarFeS” and “Base” scenarios.

References

- Chen, Q., Wang, X., Fu, X., Li, X., Alexander, B., Peng, X., Wang, W., Xia, M., Tan, Y., Gao, J., Chen, J., Mu, Y., Liu, P., and Wang, T.: Impact of molecular chlorine production from aerosol iron photochemistry on atmospheric oxidative capacity in North China, *Environ. Sci. Technol.*, 58, 12585-12597, doi: 10.1021/acs.est.4c02534, 2024.
- Hamilton, D., Scanza, R., Yan, F., Guinness, J., Kok, J., Li, L., Liu, X., Rathod, S., Wan, J. S., Wu, M., and Mahowald, N.: Improved methodologies for Earth system modelling of atmospheric soluble iron and observation comparisons using the Mechanism of Intermediate complexity for Modelling Iron (MIMI v1.0), *Geosci. Model Dev.*, 12, 3835-3862, doi: 10.5194/GMD-12-3835-2019, 2019.
- Luo, C., Mahowald, N., Bond, T., Chuang, P. Y., Artaxo, P., Siefert, R., Chen, Y., and Schauer, J.: Combustion iron distribution and deposition, *Glob. Biogeochem. Cycle*, 22, GB1012, doi: 10.1029/2007gb002964, 2008.
- Meidan, D., Li, Q. Y., Cuevas, C. A., Doney, S. C., Fernandez, R. P., van Herpen, M., Johnson, M. S., Kinnison, D. E., Li, L. L., Hamilton, D. S., Saiz-Lopez, A., Hess, P., and Mahowald, N. M.: Evaluating the potential of iron-based interventions in methane reduction and climate mitigation, *Environ. Res. Lett.*, 19, doi: 10.1088/1748-9326/ad3d72, 2024.
- Meskhidze, N., Chameides, W. L., and Nenes, A.: Dust and pollution: A recipe for enhanced ocean fertilization?, *J Geophys Res-Atmos*, 110, D03301, doi: 10.1029/2004jd005082, 2005.
- Myriokefalitakis, S., Tsigaridis, K., Mihalopoulos, N., Sciare, J., Nenes, A., Kawamura, K., Segers, A., and Kanakidou, M.: In-cloud oxalate formation in the global troposphere: a 3-D modeling study, *Atmos. Chem. Phys.*, 11, 5761-5782, doi: 10.5194/acp-11-5761-2011, 2011.
- Pennacchio, L., van Herpen, M., Meidan, D., Saiz-Lopez, A., and Johnson, M. S.: Catalytic efficiencies for methane removal: Impact of HOx, NOx, and chemistry in the high-chlorine regime, *ACS Earth Space Chem.*, 9, 504-512, doi: 10.1021/acsearthspacechem.4c00283, 2025.
- Röckmann, T., van Herpen, M., Brashear, C., van der Veen, C., Gromov, S., Li, Q. Y., Saiz-Lopez, A., Meidan, D., Barreto, A., Prats, N., Marmol, I., Ramos, R., Banos, I., Arrieta, J. M., Zaehle, S., Jordan, A., Moossen, H., Timas, H., Young, D., Sperlich, P., Moss, R., and Johnson, M. S.: The use of $\delta^{13}\text{C}$ in CO to determine removal of CH₄ by Cl radicals in the atmosphere, *Environ. Res. Lett.*, 19, doi: 10.1088/1748-9326/ad4375, 2024.
- Scanza, R., Hamilton, D., García-Pando, C. P., Buck, C., Baker, A., and Mahowald, N.: Atmospheric processing of iron in mineral and combustion aerosols: development of an intermediate-complexity mechanism suitable for Earth system models, *Atmos. Chem. Phys.*, 18, 14175-14196, doi: 10.5194/ACP-18-14175-2018, 2018.
- van Herpen, M., Li, Q. Y., Saiz-Lopez, A., Liisberg, J. B., Röckmann, T., Cuevas, C. A., Fernandez, R. P., Mak, J. E., Mahowald, N. M., Hess, P., Meidan, D., Stuut, J. B. W., and Johnson, M. S.: Photocatalytic chlorine

atom production on mineral dust-sea spray aerosols over the North Atlantic, *Proc. Natl. Acad. Sci. U.S.A.*, 120, e2303974120,doi: 10.1073/pnas.2303974120, 2023.

Yuan, T., Song, H., Oreopoulos, L., Wood, R., Bian, H., Breen, K., Chin, M., Yu, H., Barahona, D., Meyer, K., and Platnick, S.: Abrupt reduction in shipping emission as an inadvertent geoengineering termination shock produces substantial radiative warming, *Commun Earth Environ*, 5, 281,doi: 10.1038/s43247-024-01442-3, 2024.